Draft version November 13, 2017
Preprint typeset using LaTeX style emulateapj v. 11/10/09

EXPANDED VERY LARGE ARRAY DETECTION OF 44.1 GHz CLASS I METHANOL MASERS IN SAGITTARIUS A

Y. M. Pihlström[1]
Department of Physics and Astronomy, University of New Mexico, MSC07 4220, Albuquerque, NM 87131

L. O. Sjouwerman
National Radio Astronomy Observatory, P.O. Box O, 1003 Lopezville Rd., Socorro, NM 87801

and

V. L. Fish
MIT Haystack Observatory, Route 40, Westford, MA 01886

Draft version November 13, 2017

ABSTRACT

We report on the detection of 44 GHz Class I methanol (CH_3OH) maser emission in the Sgr A complex with the Expanded Very Large Array (EVLA). These EVLA observations show that the Sgr A complex harbors at least four different tracers of shocked regions in the radio regime. The 44 GHz masers correlate with the positions and velocities of previously detected 36 GHz CH_3OH masers, but less with 1720 MHz OH masers. Our detections agree with theoretical predictions that the densities and temperatures conducive for 1720 MHz OH masers may also produce 36 and 44 GHz CH_3OH maser emission. However, many 44 GHz masers do not overlap with 36 GHz methanol masers, suggesting that 44 GHz masers also arise in regions too hot and too dense for 36 GHz masers to form. This agrees with the non-detection of 1720 MHz OH masers in the same area, which are thought to be excited under even cooler and less dense conditions. We speculate that the geometry of the 36 GHz masers outlines the current location of a shock front.

Subject headings: Galaxy: center — ISM: clouds — ISM: supernova remnants — Masers — Shock waves — Supernovae: individual(Sgr A East)

1. INTRODUCTION

The Sagittarius A complex is one of the best studied regions in the sky and encompasses several interesting phenomena like the nearest supermassive nuclear black hole (Sgr A*), the Circumnuclear Disk (CND), star forming regions (SFRs) and supernova remnants (SNRs). The line of sight toward the Sgr A complex consists of the SNR Sgr A East in the back and the CND (whose ionized part is known as Sgr A West) in the front partly overlapping with Sgr A East. Molecular gas is abundant and well distributed; the CND consists of irregularly distributed clumps of molecular gas and there are two giant molecular cloud cores (GMCs) called the +20 and $+50\,\mathrm{km\,s^{-1}}$ clouds (M−0.13−0.08 and M−0.02 − 0.07 respectively). These GMCs form the molecular belt stretching across the Sgr A complex, providing the interstellar medium (ISM) that interacts with Sgr A East. A nice and recent comprehensive overview is presented by Amo-Baladrón et al. (2011).

Bright maser lines are useful probes of physical conditions within molecular clouds, especially when mapped in detail by interferometers. One example is the collisionally pumped 1720 MHz OH maser which is widely recognized as a tracer for shocked regions, observed both in SFRs and SNRs. In SNRs, Very Large Array (VLA) observations have shown they originate in regions where the shocks collide with the interstellar medium (e.g. Claussen et al. 1997; Yusef-Zadeh et al. 2003; Frail & Mitchell 1998). Such OH masers are numerous in Sgr A East, thus probing the conditions of the interaction regions between the +50 and $+20\,\mathrm{km\,s^{-1}}$ clouds and the SNR Sgr A East.

Dense gas structures in the Galactic center region, including Sgr A East, are traced by ammonia and methanol thermal emission (Coil & Ho 2000; Szczepanski et al. 1989, 1991). Methanol abundances are high enough to produce maser emission. Like 1720 MHz OH masers, Class I methanol masers such as the 36 and 44 GHz transitions are excited through collisions. Theoretical modeling of collisional OH excitation predicts that the 1720 MHz OH should be found in regions of $n \geq 10^5$ cm^{-3} and $T \sim 75\,\mathrm{K}$ (Gray et al. 1991, 1992; Wardle 1999; Lockett et al. 1999; Pihlström et al. 2008). The number density and temperature required for 36 GHz methanol masers are near those modeled for 1720 MHz OH masers, with $n \sim 10^4 - 10^5$ cm^{-3} and $T < 100\,\mathrm{K}$ (Morimoto et al. 1985; Cragg et al. 1992; Liechti & Wilson 1996). At least in SFRs, higher densities and temperatures of $n \sim 10^5 - 10^6$ cm^{-3} and $T = 80 - 200\,\mathrm{K}$ will optimize the maser output for the Class I 44 GHz line, while the 36 GHz maser eventually becomes quenched (Sobolev et al. 2005, 2007; Pratap et al. 2008). Finding these methanol maser lines may therefore help to constrain the upper limit of the density in the shocked SNR regions. In turn such limits can be used to estimate the importance of compression by shocks in the formation of stars near SNRs.

That Class I methanol maser lines are detectable

ylva@unm.edu
[1] Y. M. Pihlström is also an Adjunct Astronomer at the National Radio Astronomy Observatory

TABLE 1
44 GHz methanol maser associations

	Position (J2000) Right Asc.	Declination	Pointing position	V_{LSR} km s^{-1}	$T_{b,44\ GHz}$ 10^3 K	Flux density[a] Jy beam^{-1} 44 GHz	36 GHz
1	17 45 38.92	−29 00 21.0	Calibrator	44.0	0.1	0.13	
2	17 45 43.94	−29 00 19.5	C, Calibrator	49.9	2.1	2.16	1.0
3[b]	17 45 49.36	−28 58 53.3	E	45.2	0.7	0.93	75.5
4[c]	17 45 49.56	−28 59 00.6	E	46.5	1.4	1.43	35.0
5	17 45 49.67	−28 58 55.2	E	42.7	2.4	2.42	
6	17 45 49.89	−28 59 04.5	E	36.9	1.4	1.47	
7	17 45 50.48	−29 00 05.0	D	49.9	0.7	0.55	36.9
8	17 45 50.48	−28 58 48.7	E	59.5	0.5	0.50	
9	17 45 50.49	−28 59 07.6	E	42.8	0.4	0.45	
10	17 45 50.65	−28 59 08.8	E	28.0	0.7	0.74	5.2
11	17 45 51.41	−28 59 10.2	E	44.2	0.5	0.45	
12	17 45 51.55	−28 58 53.7	E	46.7	0.5	0.51	
13	17 45 51.62	−28 58 26.5	E	52.7	0.6	0.56	
14	17 45 51.88	−28 58 52.9	E	47.1	2.3	2.39	15.9
15[c]	17 45 52.12	−28 58 55.4	E	45.9	0.6	0.64	11.3
16	17 45 52.16	−28 58 22.3	E	55.4	1.1	1.11	
17	17 45 52.43	−28 58 58.2	E	43.7	0.6	0.58	
18	17 45 52.55	−28 58 56.8	E	45.7	0.6	0.60	

[a] Maser peak flux density in the channel of maximum flux; highly unreliable for masers 2, 13 and 16 detected beyond the primary beam. The 36 GHz peak fluxes are from the data from Sjouwerman et al. (2010).
[b] Brightest component in a cluster of detections.
[c] Multiple spectral features detected at the same position.

in SNR/cloud interaction regions was shown by Sjouwerman et al. (2010), using the 7 first antennas outfitted with 36 GHz receivers at the Expanded VLA (EVLA, Perley et al. (2011)). Several bright masers were found near the 1720 MHz OH masers in the Sgr A East molecular cloud - SNR interaction region; a feature also observed by many others (e.g. Tsuboi et al. 2009). To test whether the relation between the collisionally excited 36 and 44 methanol masers and 1720 MHz OH holds in general, we here present the result of a search for Class I 44 GHz methanol maser emission in the Sgr A region.

2. OBSERVATIONS

On 2010 October 16, the EVLA was used in its C configuration to observe the $J = 7_0 \rightarrow 6_1 A^+$ rotational transition of CH_3OH at 44 069.41 MHz as part of observing project 10B-146. The complete results on all sources will be reported elsewhere; here we concentrate on the emission detected in the Sgr A region. The new Observation Preparation Tool (OPT) was used to schedule the observations with a bandwidth of 8 MHz in dual polarization. The bandwidth was split in 256 channels with a resulting velocity resolution of approximately 0.2 km s^{-1} over a total velocity coverage of 51 km s^{-1}. At the time of the observations full Doppler tracking was not available, but instead the sky frequency was calculated at the beginning of each scheduling block (observing run) and then kept fixed throughout the observation. Velocity errors due to uncorrected Doppler effects over the length of a scan are much less than the channel width. We note that both maser and thermal emission may be detected when observing in the C-configuration (see Sec. 3).

The primary beam at 44 GHz is about 56″, and the full Sgr A region could not be covered by a single pointing. We selected five pointing positions ("A" through "E", see Fig. 1) with central velocities based on previous results on 1720 MHz OH masers and 36 GHz methanol masers. Position A corresponds to a region of high-velocity 1720 MHz OH masers belonging to the circumnuclear disk, covering LSR velocities between 106 and 157 km s^{-1}. In position B we previously detected 36 GHz methanol masers at velocities around 23 km s^{-1} (LSR coverage −3 to +39 km s^{-1}). This pointing position partly overlaps on the sky with pointing position C which has a central velocity of 48 km s^{-1} (LSR coverage 22 – 74 km s^{-1}) based on the 1720 MHz OH masers. Finally, positions D and E correspond to a region where the 50 km s^{-1} molecular cloud interacts with Sgr A East, and where 1720 MHz masers are numerous. The LSR velocity coverage for these pointing positions was 22 – 74 km s^{-1}. As a bonus we could include the pointing on our calibrator Sgr A* and investigate the same velocity ranges in this part of the sky.

The data were reduced using standard procedures in AIPS, using 3C 286 as the flux density calibrator resulting in a typical flux density uncertainty of 15%. In the fields were masers were found, a strong maser channel was used for self-calibration, with its solutions applied to all channels. Each cube was CLEANed with robust weighting down to a level of five times the theoretical rms over a field approximately twice the primary beam. This was necessary since some masers appeared in the sidelobes and needed to be accounted for in the CLEANing process. The resulting typical channel rms noise is 15 – 20 mJy/beam, and the restoring beam is 1.3″×0.5″. Peak fluxes are corrected for primary beam attenuation using AIPS task PBCOR.

3. RESULTS

The image cubes were searched for masers, and parameters for the individual features were extracted using the AIPS task JMFIT. The combined results are presented in Table 1 for spectral features with peak flux densities exceeding 10 times the rms noise. A few weaker masers

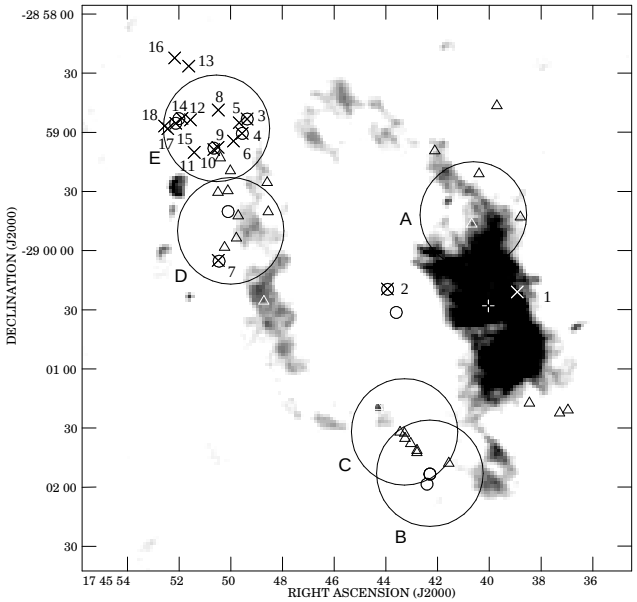

FIG. 1.— Relative positions of the 44 GHz methanol masers (crosses), 36 GHz methanol masers (circles) and 1720 MHz OH masers (triangles). The big circles show the five main field-of-view positions A through E covered. The plus symbol marks the position of Sgr A*, which is an extra field that could be examined for 44 GHz methanol masers. A blow-up of the upper left region is shown in Fig. 2.

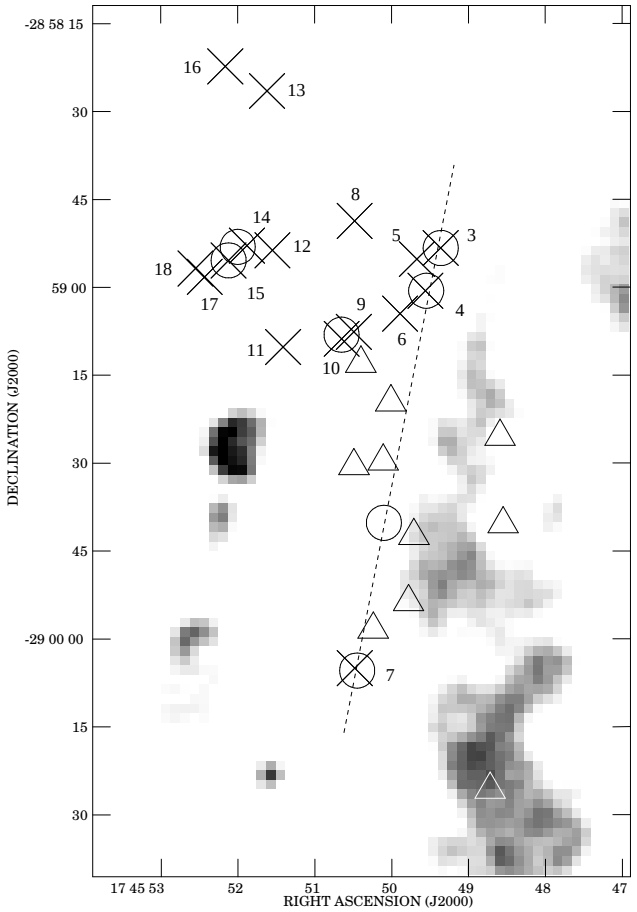

FIG. 2.— A zoom in of the northeast region of Fig. 1, showing an apparent systematic offset in the location of the three maser species, with the 44 GHz methanol masers concentrated to the northeast, the 1720 MHz OH masers more to the southwest and a NNW-SSE line of (four) 36 GHz methanol masers, three co-spatial with 44 GHz, roughly dividing the two regions. The dashed line shows the alignment of 36 GHz masers with the shockfront in the NNW-SSE direction.

exist in the cubes, but they are all located close to the brighter masers in position and velocity, and will not change any of the discussion in Sect. 4.

A few features show more than one spectral peak at a given position, implying there is structure on scales smaller than the EVLA beam. Some spectral features have wings of weaker emission extending over 6 – 8 km s^{-1}. Since the observations were taken when the EVLA was in C-configuration, we suspect that some of this broad and weak emission is of thermal origin. The peak flux density of the spectral features corresponds to brightness temperatures exceeding 10^3 K, indicating that at least some of these features are masers. A definite confirmation of this needs higher angular resolution observations. However, several features are co-located spatially and spectrally with previously detected 36 GHz methanol emission confirmed to be masers (Sjouwerman et al. 2010). Both the 44 GHz and 36 GHz masers are thought to be excited by the same process, so it is likely the 44 GHz observed here is maser emission even though a smaller fraction of the emission may be of thermal origin.

Three masers were detected outside the primary beam (2, 13 and 16 in Table 1) and their flux density is therefore less certain than for masers located within the primary beam. The position and velocity of maser 2 at 50 km s^{-1} agrees very well with the position of a 36 GHz maser at 51 km s^{-1} (Sjouwerman et al. 2010), and therefore increases our confidence in this detection. This 44 GHz maser has previously been reported on by Yusef-Zadeh et al. (2008), and is associated with a molecular clump 'G'. Similarly, we confirm their maser 'V' (our maser 1) in our data taken for the phase-reference calibrator J1745−2900 (i.e. Sgr A*), and both 'G' and 'V' in archival VLA data taken on 2009 April 23. The 44 GHz maser associated with clump 'F' reported by Yusef-Zadeh et al. (2008) is not confirmed by our, nor the archival, observations. The additional two masers detected outside the primary beam, 13 and 16, also do not have 36 GHz masers directly associated with them.

Figure 1 plots the position of the detected 44 GHz methanol sources compared to the previously detected 36 GHz and 1720 MHz OH masers. Also indicated are the spatial regions, primary beams A through E, selected for maser searches in these observations. Figure 2 shows the northeast region of Sgr A East where most 44 GHz masers are located. From these plots a few main results can be concluded. Firstly, the positions and velocities of several 44 GHz masers (2, 3, 4, 7, 10, 14, and 15 from Table 1) agree to within the errors with the values reported by Sjouwerman et al. (2010) for the 36 GHz masers. Secondly, there is a systematic difference between the overall distributions of the 1720 MHz OH, 36 GHz methanol and 44 GHz methanol masers. In the northeast (upper left) region, in overlap with the densest part of the 50 km s^{-1}

cloud, the 44 GHz masers are offset to the northeast with respect to a narrow, almost linear southsoutheast to northnorthwest distribution of the 36 GHz masers. The 1720 MHz OH masers are found on the other side of the 36 GHz masers, near the radio continuum of the SNR to the southwest (lower right). An offset between the OH and methanol is also observed in the southeastern interaction region, where the SNR G359.02–0.09 overlaps the Sgr A East continuum (Coil & Ho 2000; Herrnstein & Ho 2005). These positional offsets are discussed further in Sect. 4.

4. DISCUSSION

To date, four collisionally excited radio frequency maser tracers have been detected in the Sgr A complex; 1720 MHz OH, 36 and 44 GHz CH_3OH and 22 GHz H_2O (Yusef-Zadeh et al. 1996; Karlsson et al. 2003; Sjouwerman & Pihlström 2008; Yusef-Zadeh et al. 2008; Sjouwerman et al. 2010). The 22 GHz water masers trace regions of higher density and temperature than are typical for the SNR/cloud interaction regions, and will not be discussed in this paper. The methanol and hydroxyl are excited under similar conditions, and in this Letter we discuss their relative positions and possible origins.

4.1. *36 GHz versus 44 GHz Methanol Masers*

Modeling of methanol masers suggest that the 36 GHz transition occurs under somewhat cooler and less dense ($T \sim 30$ – 100 K, $n \sim 10^4 - 10^5$ cm^{-3}) conditions than the 44 GHz transition ($T \sim 80$ – 200 K, $n \sim 10^5 - 10^6$ cm^{-3}; see, e.g. Pratap et al. (2008)). The range of physical conditions do however overlap, and some spatial overlap could therefore be expected. Seven 44 GHz masers (2, 3, 4, 7, 10, 14 and 15) show an almost perfect overlap in both position and velocity with 36 GHz masers (Sjouwerman et al. 2010). Here, according to the modeling, the densities and temperatures should be close to 10^5 cm^{-3} and 100 K to produce both methanol maser lines.

It is striking that the brightest 36 GHz masers, all in positions D and E (Sjouwerman et al. 2010), are narrowly distributed along a line roughly from north to south, of which three coincide with 44 GHz masers (3, 4 and 7) in position and velocity within the errors. This NNW-SSE division more or less coincides with the sharp gradient in low-frequency radio continuum emission of the Sgr A East SNR (Pedlar et al. 1989) and appears to be located in the sheath in the CS emission as mapped by Tsuboi et al. (2009). The mean velocity of each transition is 46 km s^{-1}, implying that they arise in similar regions of the molecular cloud where the velocities still are less disturbed by the SNR shock (see Sect. 4.2). Apart from two individual exceptions located far from this area (1 and 2), we do not find any 44 GHz (nor 36 GHz) masers westward of this line in our pointings. It is therefore tempting to speculate that the line delineates the arrival of the shock front, where enough material has been swept up to provide the density for the creation of (very bright 36 GHz) methanol masers, but not yet enough energy has dissipated to dissociate all methanol or to significantly disturb the velocity structure by means of a reverse shock (Section 4.2). That the 36 GHz masers appear to be much brighter than the 44 GHz masers may be due to the smaller synthesized beams in the 36 GHz observations (200-400 mas using B-configuration). However, within each observation, the masers outlining the shock front on average are at least twice as bright as the other masers in the same transition. It suggests that the geometry of the shock front, moving in the plane of the sky, causes the path length amplification to be largest in the line of sight, hence lending support to our speculation.

In the northeastern part of Sgr A East toward the core of the 50 km s^{-1} cloud, there is a group of 44 GHz masers with a distinct positional offset from the NNW-SSE line of 36 GHz masers, and which have no accompanying 36 GHz masers. The narrower distribution of 36 GHz masers suggests that the conditions required to produce masers in this transition are not fulfilled to the same extent further to the northeast. The position of the 36 GHz emission is consistent with being just in the SNR/cloud interaction region, while the 44 GHz masers may be found deeper inside the denser parts of the cloud where 36 GHz masers are quenched. This situation has been found in sites of massive star formation, where the 44 GHz masers typically are brighter than the 36 GHz masers (e.g. Pratap et al. 2008; Fish et al. 2011), suggesting some of the 44 GHz masers may be associated with star formation. The lack of companion 36 GHz masers in this putative star-forming region in the northeast corner of Sgr A East (e.g. Tsuboi et al. 2009) therefore may be due to the limited sensitivity of the 36 GHz observations. This picture, at least for this region in the Galactic center, in which 44 GHz masers are primarily associated with cloud cores and 36 GHz masers are found at the boundaries of the SNR interaction regions, is consistent with theoretical models indicating that 44 GHz masers can be produced at higher densities than 36 GHz masers. The existence of 36 GHz masers without accompanying 44 GHz masers in positions B and C may then indicate the interaction region of two SNRs without the presence of a dense cloud core.

4.2. *OH versus Methanol Masers*

As is the case with Class I methanol masers, 1720 MHz OH masers are used as tracers of shocked regions. The presence of 1720 MHz OH masers indicates the presence of C-shocks (e.g. Lockett et al. 1999). Modeling of OH and CH_3OH shows that the three maser transitions discussed here require similar densities and temperatures. This agrees well with the detection of all three masers in Sgr A East. However, we observe a distinct offset in positions between the methanol and OH masers (Fig. 1). In the northeast interaction region between the 50 km s^{-1} cloud and Sgr A East the OH masers are found more to the southwest. In addition, the 1720 MHz OH masers have a slightly higher mean velocity of 57 km s^{-1} versus 46 km s^{-1} for the methanol. We do note however, that the 1720 MHz OH does overlap in the sky with the line of 36 GHz masers.

A similar offset is observed in the southeastern interaction region in pointing positions B and C, where the methanol masers are offset southwest from the OH. The OH mean velocities here are 58 km s^{-1} to be compared to the 24.5 km s^{-1} for the 36 GHz methanol. No 44 GHz methanol was detected in this region.

The association between 1720 MHz OH and 36 GHz methanol emission may be due to the processes that form these molecules. OH is created by dissociation of H_2O (and maybe also CH_3OH), and the propagation of a C-shock creates densities and temperatures suitable for 1720 MHz OH inversion and probably also some Class I methanol emission (e.g. Lockett et al. 1999; Draine et al. 1983). Thus, OH masers should preferentially be found in the SNR post-shock region. This agrees with the OH masers being co-located with positions of radio continuum, outlining regions where electrons have been accelerated by the shock. The production of methanol is less well understood, but it is believed that methanol is released from grain mantles, either by sputtering from a shock or by evaporation when temperatures above 100 K are reached (Hidaka et al. 2004; Menten et al. 2009; Bachiller & Perez Gutierrez 1997; Voronkov et al. 2006; Hartquist et al. 1995). For OH, modeling shows that a temperature around 50-125 K and a density of $10^5 \mathrm{cm}^{-3}$ will be conducive to OH inversion (Lockett et al. 1999; Wardle 1999; Pihlström et al. 2008). This range of values agrees with both 36 GHz and 44 GHz methanol production, but non-detections of 6 GHz and higher frequency OH maser transitions in SNRs like Sgr A East (Fish et al. 2007; Pihlström et al. 2008; McDonnell et al. 2008) imply the densities and temperatures are biased towards the lower values, perhaps specifically favoring 36 GHz masers to have a closer spatial connection with 1720 MHz OH masers.

5. CONCLUSIONS

The methanol and OH masers found in the Sgr A complex are located near each other but are not co-spatial, indicating they trace different shocks or different regions of the shock. By comparing velocities of the methanol and the OH we argue that the methanol is tracing material that has been less disturbed by the shocks, while the OH is located further in the postshock gas. The narrow, collinear distribution of 36 GHz methanol in the Sgr A East interaction region with the $50\,\mathrm{km\,s^{-1}}$ cloud aligns with the SNR shock front, while the OH is more widely spread into the post-shock regions. 44 GHz and 36 GHz methanol maser overlaps occur in the cloud/SNR shock region where the conditions for maser action in both lines are fulfilled. Deeper in the $50\,\mathrm{km\,s^{-1}}$ cloud core, there is a group of 44 GHz methanol masers observed with no accompanying bright 36 GHz masers, indicating a hotter and denser environment than the material swept up from the shock. These masers are likely to trace star formation within the cloud core.

The limited number of pointing positions in addition to a limited velocity coverage makes it hard to in detail determine the relationship between the methanol and OH masers. New data mapping a more complete region of Sgr A is underway, and we are aiming for a similar study with a broader velocity range when the EVLA upgrade is complete.

Facilities: EVLA.

REFERENCES

Amo-Baladrón, M. A., Martín-Pintado, J., & Martín, S. 2011, A&A, 526, A54

Bachiller, R., & Perez Gutierrez, M. 1997, ApJ, 487 L93

Claussen, M. J., Frail, D. A., Goss, W. M., & Gaume, R. A. 1997, ApJ, 489, 143

Coil, A. L., & Ho, P. T. P. 2000, ApJ, 533, 245

Cragg, D. M., Johns, K. P., Godfrey, P. D., & Brown, R. D. 1992, MNRAS, 259, 203

Draine, B. T., Roberge, W. G., & Dalgarno, A. 1983, ApJ, 264, 485

Fish, V. L., Sjouwerman, L. O., & Pihlström, Y. M. 2007, ApJ, 670, L117

Fish, V. L., Muehlbrad, T. C., Pratap, P., Sjouwerman, L. O., Strelnitski, V., Pihlström, Y. M., & Bourke, T. L. 2011, ApJ, 729, 14

Frail, D.A., & Mitchell, G.F. 1998, ApJ, 508, 690

Gray, M. D., Doel, R. C., & Field, D. 1991, MNRAS, 262, 30

Gray, M. D., Field, D., & Doel, R. C. 1992, A&A, 264, 220

Hartquist, T. W., Menten, K. M., Lepp, S., & Dalgarno, A. 1995, MNRAS, 272, 184

Herrnstein, R. M., & Ho, P. T. P. 2005, ApJ, 620, 287

Hidaka, H., Watanabe, N., Shiraki, T. M. Nagaoka, A., & Kouchi, A. 2004, ApJ, 614, 1124

Karlsson, R., Sjouwerman, L. O., Sandqvist, A., & Whiteoak, J. B. 2003, A&A, 403, 1011

Liechti, S., & Wilson, T.L. 1996, A&A, 314, 615

Lockett, P., Gauthier, E., & Elitzur, M. 1999, ApJ, 511, L235

McDonnell, K. E., Wardle, M., & Vaughan, A. E. 2008, MNRAS, 390, 49

Menten, K. M., Wilson, R. W., Leurini, S., & Schilke, P. 2009, ApJ, 692, 47

Morimoto, M., Kanzawa, T., & Ohishi, M. 1985, ApJ, 288, L11

Pedlar, A., Anantharamaiah, K. R., Ekers, R. D., Goss, W. M., van Gorkom, J. H., Schwarz, U. J., & Zhao, J.-H. 1989, ApJ, 342, 769

Perley, R. A., Chandler, C. J., Butler, B. J., & Wrobel, J. M. 2011, ApJ, in press

Pihlström, Y. M., Fish, V. L., Sjouwerman, L. O., Zschaechner, L. K., Lockett, P. B., & Elitzur, M. 2008, ApJ, 676, 371

Pratap, P., Shute, P. A., Keane, T. C., Battersby, C., & Sterling, S. 2008, AJ, 135, 1718

Szczepanski, J. C., Ho, P. T. P., Haschick, A. D., & Baan, W. A. 1989, IAU Symp. 136, 383

Szczepanski, J. C., Ho, P. T. P., & Gusten, R. 1991, ASP Conf. Series, Vol. 16, 143

Sjouwerman, L. O., Pihlström, Y. M., & Fish, V. L. 2010, ApJ, 710, L111

Sjouwerman, L. O., & Pihlström, Y. M. 2008, ApJ, 681, 1287

Sobolev, A. M., Ostrovskii, A. B., Kirsanova, M. S., Shelemei, O. V., Voronkov, M. A., & Malyshev, A. V. 2005, in IAU Symp. 227, Massive star birth: A crossroads of Astrophysics, ed. R. Cesaroni, M. Felli, E. Churchwell & M. Walmsley (Cambridge: Cambridge Univ. Press) 174

Sobolev, A. M. et al. 2007, in IAU Symp. 242, Astrophysical Masers and their Environments, ed. A. Vazdekis & R. Peletier (Cambridge: Cambridge Univ. Press) 81

Tsuboi, M., Miyazaki, A., & Okumura, S. K. 2009, PASJ, 61, 29

Voronkov, M. A., Brooks, K. J., Sobolev, A. M., Ellingsen, S. P., Ostrovskii, A. B., & Caswell, J. L. 2006, MNRAS, 373, 411

Wardle, M. 1999, ApJ, 525, L101

Yusef-Zadeh, F., Braatz, J., Wardle, M., & Roberts, D. 2008, ApJ, 683, L147

Yusef-Zadeh, F., Wardle, M., Rho, J., & Sakano, M. 2003, ApJ, 585, 319

Yusef-Zadeh, F., Roberts, D. A., Goss, W. M., Frail, D. A., & Green, A. J. 1996, ApJ, 466, L25